PHYSICAL REVIEW A VOLUME 35, NUMBER 1 JANUARY 1, 1987

Symmetry breaking and metastable chaos in a coherently driven superradiant system

V. G. Benza
Dipartimento di Fisica, Università degli Studi di Milano, via Celoria 16, I-20133 Milano, Italy and Istituto Nazionale di Fisica Nucleare, Sezione di Milano, I-20133 Milano, Italy

S. W. Koch
Optical Sciences Center and Physics Department, University of Arizona, Tucson, Arizona 85721
(Received 19 May 1986)

The temporal evolution of the transmitted light field is computed for a high-density gas of two-level atoms, which is externally excited by an amplitude-modulated field in resonance with the atomic transitions. The transmitted field is shown to exhibit a chaotic transient and a cascade through different phase-locked orbits. Due to the asymmetry of these orbits, the field develops a nonzero average value even in the absence of a bias.

I. INTRODUCTION

In the last few years, the dynamic response of a driven, damped pendulum has been studied quite intensively,[1] and by now this model serves as a paradigmatic example of chaotic dynamics. The attraction of this system is based on both its mathematical simplicity and its physical relevance. Particularly, the driven damped pendulum has been shown to be a quite realistic model for a Josephson junction, and as a consequence of this connection, Josephson junctions are now an important experimental instrument to test the theoretical predictions of chaotic behavior.

In this paper, we discuss an example of a quantum-optics system, which in some idealization can also be described by the damped pendulum equation. Starting from the corresponding predictions for the chaotic pendulum dynamics, we eliminate some of the idealizing assumptions and study the changes in the dynamic response for the more realistic model.

In fact, the pendulum model is widely used in the field of quantum optics to describe the interaction between a gas of two-level atoms and the electromagnetic field.[2] Here the pure pendulum equation applies if one discusses the coupling of the two-level system to a single field mode at resonance with the atomic transitions. One neglects both the cavity losses and the atomic decay processes. Nevertheless, this model can be used under certain circumstances and it has been applied quite successfully, e.g., to predict the effect of squeezing,[3] i.e., the anisotropy of the variances of the components of the transmitted electromagnetic field.

In the more general case, an optical two-level system is described by the Maxwell-Bloch equations. In comparison to the pure pendulum, this amounts to an extension of the phase space from two to at least three dimensions. Such a complication is, however, unavoidable if one wants to investigate also the effects caused by finite atomic damping. In this paper, we especially address the question of whether a more realistic model of the two-level system follows a similar route to chaotic behavior as would be predicted for a pure pendulum. In more physical terms, we investigate the dynamics of a superradiant system under the influence of a periodically modulated external field. We examine the parameter space, where the pure pendulum model shows the quasiperiodicity route to chaos. We are mostly concerned about the influence of the physically unavoidable atomic damping on the dynamic output.

For the external driving field we assume a laser beam which is at resonance with the atomic transitions and with the cavity. As is well known, a study of the possible approach to chaos in the transmitted field requires an externally controllable frequency which competes with the internal dynamics. Therefore, we assume that the driving laser is amplitude modulated with a frequency of the order of the oscillation frequency of the nonlinear medium. This situation is chosen because without atomic damping one can model it directly by the equation of the driven pendulum where the driving force is the amplitude of the injected signal.

Chaos in optical systems has been studied, among other cases, both theoretically[4(a)] and experimentally[4(b)] for the example of an active (laser) medium which is pumped by a time-dependent external field. This example, however, differs significantly from our case, since we are dealing with a passive medium in which the atomic cooperativity plays an important role in the frequency-mismatch phenomena. Taking advantage of the connection of our model with the driven pendulum, we will describe the dynamics in terms of simple two-dimensional phase portraits, leaving a complete statistical analysis for future work.

This paper is organized as follows. In Sec. II we introduce the physical system and the Maxwell-Bloch equations and recall some known results from the driven pendulum. In Sec. III we describe the numerical results in the case in which the driving term is purely oscillatory (zero bias). In Sec. IV we give an analytical description of the system. In Sec. V we report on other numerical results in the presence of bias, and in Sec. VI we make some comments and point out some open problems.

II. MAXWELL-BLOCH EQUATIONS

We consider a gas of N two-level atoms of frequency ω_0 contained in a cavity at resonance with the atomic transitions. We limit ourselves to a single-mode description, and assume a homogeneously broadened medium. As is well known, for sufficiently large N such a system is characterized by cooperative behavior. The atoms exchange energy with the field mode through nonliner oscillations, provided the dephasing processes of the atoms occur on time scales large enough with respect to the period of such oscillations.

The period is given in terms of the so-called cooperation time $\tau_c=(gN^{1/2})^{-1}$ (Ref. 5), g being the dipole coupling constant. We introduce in the system a new frequency, competing with τ_c^{-1}, in the following way. We inject in the cavity a coherent beam with resonant frequency ω_0, but with modulated amplitude. The frequency of this modulation is taken to be of the order τ_c^{-1}. Denoting by E the field amplitude, by D the population difference, and by A the amplitude of the injected signal, which we will assume of the general form $A(t)=A_0+A_1\cos(\omega_D t)$, we have the well-known Maxwell-Bloch equations

$$\begin{aligned}\frac{dP}{dt}&=2gED-\gamma_\perp P\ ,\\ \frac{dD}{dt}&=-2gEP-\gamma_{||}(D-\tfrac{1}{2}N)\ ,\\ \frac{dE}{dt}&=-k[E-A(t)]-gP\quad g=\left[\frac{\omega_0\mu^2}{\hbar V}\right]^{1/2}\ ,\end{aligned}\tag{2.1}$$

where k is the inverse lifetime of the photons in the cavity, $\gamma_\perp$ and $\gamma_{||}$ are the transverse and longitudinal relaxation times, respectively, V is the volume of the cavity, and μ is the atomic dipole moment. For $A_1=0$, system (2.1) reduces to the Bonifacio-Lugiato model of optical bistability.[6] In order to compare the behavior of our system with previous analyses of the forced damped pendulum, it is convenient to rescale the variables as follows:

$$\begin{aligned}&t\to\tau=\frac{t}{\tau_c},\quad P\to p=\frac{P}{N/2},\quad D\to d=\frac{D}{N/2}\ ,\\ &E\to e=\frac{E}{N^{1/2}},\quad A\to a=\frac{A}{N^{1/2}}\ ,\end{aligned}\tag{2.2}$$

thus obtaining

$$\begin{aligned}\dot p&=2ed-\gamma'_\perp p\ ,\\ \dot d&=-2ep-\gamma'_{||}(d-1)\ ,\\ \dot e&=-k'(e-a)-\tfrac{1}{2}p\ ,\end{aligned}\tag{2.3}$$

where the derivatives are taken with respect to τ, $\gamma'_{\perp,||}=\gamma_{\perp,||}\tau_c$, $k'=k\tau_c$, and $a=a(\tau)=a_0+a_1\cos(\omega'_D\tau)$ $(\omega'_D=\omega_D\tau_C)$. If one disregards the atomic dampings the first two equations describe a rotation. Denoting $p=\rho\sin\theta$, $d=\rho\cos\theta$, and $2e=d\theta/d\tau$ one obtains, in this case, the forced damped pendulum equation

$$\frac{d^2\theta}{d\tau^2}+k'\frac{d\theta}{d\tau}+\rho\sin\theta=2k'[a_0+a_1\cos(\omega'_0\tau)]\ ,\tag{2.4}$$

which, upon the rescaling $\tau\to\bar\tau=\tau\rho^{1/2}$, $k'\to\bar k=k'/\rho^{1/2}$, and $\omega'_D\to\bar\omega_D=\omega'_D/\rho^{1/2}$ reduces to the normalized form examined by D'Humiéres *et al.*,[1(c)] with a bias $\gamma_0=2k'a_0/\rho$ and a driving amplitude $\gamma_1=2k'a_1/\rho$:

$$\ddot\theta+\bar k\dot\theta+\sin\theta=\gamma_0+\gamma_1\cos(\bar\omega_D\bar\tau)\ .\tag{2.5}$$

In the absence of atomic damping the quantity $\rho^2=p^2+d^2$ is conserved. Therefore, the dynamics described by (2.3) always maps to the pendulum equation (2.5), provided the control parameters γ_0, γ_1, $\bar\omega_D$, and $\bar k$ are rescaled according to the initial values: $\rho=[p^2(0)+d^2(0)]^{1/2}$.

We have numerically integrated the full system (2.3) by means of a 5th order Nordsieck-Gear algorithm;[7] the accuracy of the integration routine has been checked by evaluating ρ at different times in the case $\gamma'_\perp=\gamma'_{||}=0$. By choosing a time step $\Delta\tau=10^{-2}$, ρ^2 was conserved with an error in 10^{-7} up to 1 500 000 time steps even in the chaotic regime. Previous attempts, made by a simple one-step integration routine, resulted in instabilities for the value of ρ, with deviations of more than 10%, as well as in an ill-defined period-doubling route; a sensitive dependence on initial conditions was also observed in the nonchaotic regime.

For the sake of completeness, we first report on some results in the case $\gamma_\perp=\gamma_{||}=0$, and zero bias. In Fig. 1 we display phase portraits (left column) in the plane (p,e), corresponding to the pendulum phase plane $(\sin\theta,\dot\theta)$, and plots of d versus p (right column) for different values of the driving amplitude γ_1, ($\gamma_1=0.5$, 0.67, 0.675, and 0.69, respectively, from top to bottom) with fixed $\bar\omega_D=0.67$, $\bar k=0.25$. The initial conditions are always such that $\rho=1$, and $e(0)=0$.

The case $\gamma_1=0.5$ [Figs. 1(a) and 1(a')] refers to small oscillations around the unperturbed steady state $d=1, p=0$ in which the atomic system is completely deexcited (all the atoms are in the ground state, $\theta=0$).

The cases $\gamma_1=0.67$ [Figs. 1(b) and 1(b')] and $\gamma_1=0.675$ [Figs. 1(c) and 1(c')] correspond to orbits of higher excitation, in which the oscillating atomic Bloch vector almost reaches the unperturbed unstable state $d=-1, p=0$ (all the atoms in the upper level, $\theta=\pi$).

A striking feature of these cases is the asymmetry of the orbits with respect to the reflection $p\to-p$, so that the time average of the polarization is different from zero. The occurrence of this phenomenon, as a precursor of the chaotic regime, has been previously stressed in the context of Josephson junctions.[1(c)]

More precisely, in this regime degeneracy occurs, so that one can observe a given asymmetrical orbit as well as its specular image $(p\to-p)$. By slightly varying the initial conditions along the curve $\rho=1$, we obtained such specular orbits.

When $\gamma_1=0.69$ [Figs. 1(d) and 1(d')] the system is chaotic [see also Ref. 1(c)]; the orbits lie very close to the separatrix in the pendulum phase plane, but with higher excitation. The Bloch vector transits through the excited state $d=-1, p=0$ with finite velocity; the phase portrait [Fig. 1(d)] again exhibits asymmetry.

Note, the Bloch vector does not follow the orbit [Fig. 1(d')] in a unidirectional sense. Most of its cycles are in-

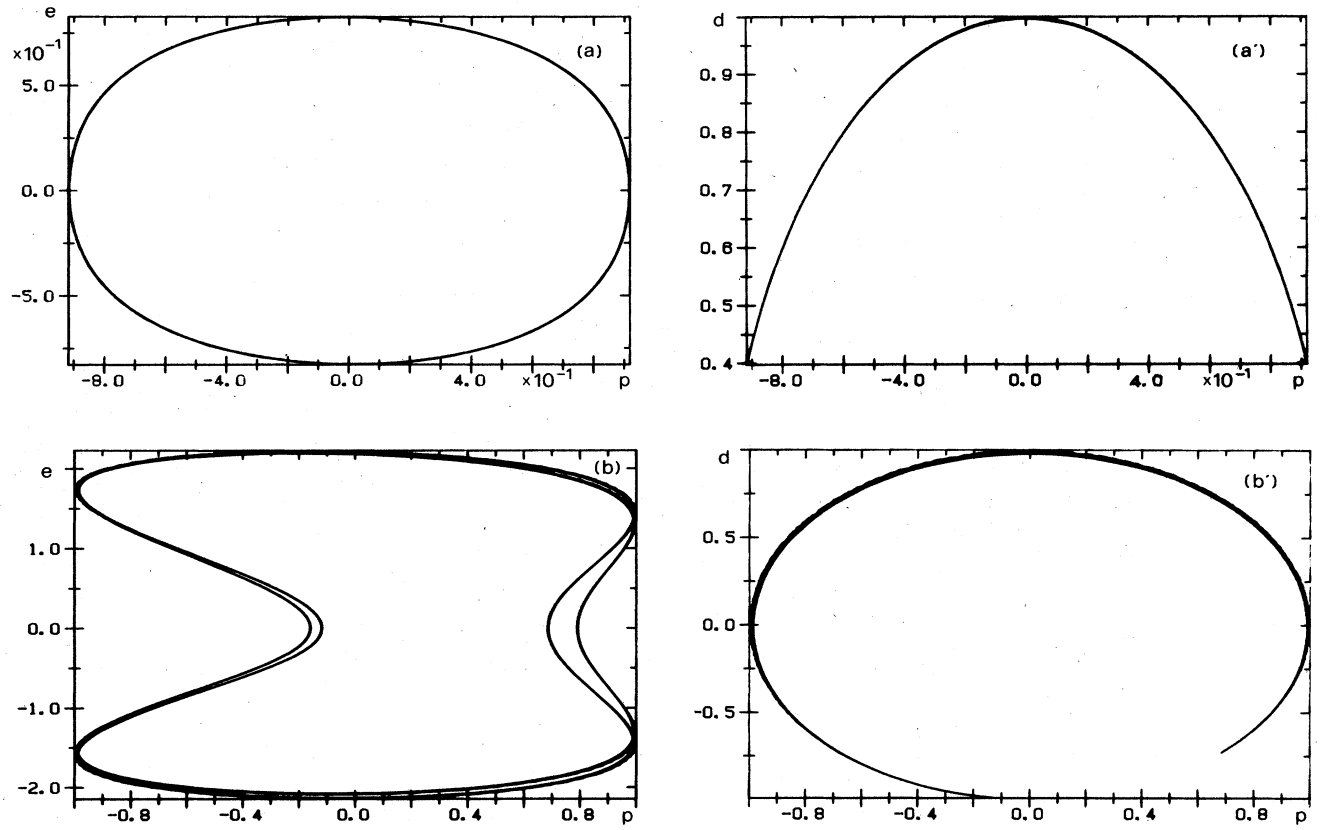

FIG. 1. Phase portraits of the solution with $\gamma'_{\perp}=\gamma'_{||}=a_0=0$, $\omega'_D=0.67$, $k'=0.25$, $e(0)=p(0)=0$, and $d(0)=1$. Left column, plane (p,e); right column, plane (p,d). γ_1 $(=2k'a_1)$ has the following values: (a,a'), 0.5; (b,b'), 0.67; (c,c'), 0.675; (d,d'), 0.69.

complete and on the average it stays much longer in the regime $d>0$ than in the regime $d<0$, as is evidenced by the respective line thickness.

III. TRANSIENT CHAOS IN THE ABSENCE OF BIAS: CASCADING THROUGH DIFFERENT PHASE-LOCKED STATES

We will now discuss some results obtained in the case without bias ($\gamma_0=0$), and finite atomic dampings, which for simplicity, are assumed to be equal ($\gamma'_{\perp}=\gamma'_{||}=\gamma$). Considering a region of control parameters corresponding to the chaotic regime in the absence of atomic dampings, we will examine the approach to steady state following the initial chaotic transient. The time behavior of the variable $\rho=(d^2+p^2)^{1/2}$ allows us to classify the different regimes of the transient in terms of stable (chaotic or phase-locked) orbits for the corresponding driven pendulum. In fact, we first note, as one easily verifies from the first two equations of (2.3), that ρ evolves on a time scale of the order of γ^{-1}. Therefore, if $\gamma \ll k'$, $\rho(\tau)$ is slowly varying with respect to $e(\tau)$, $\rho(\tau)$, and $d(\tau)$, and, apart from corrections of order γ, again system (2.3) can be mapped in Eq. (2.5).

The parameters $\bar{k}$, γ_1, and $\bar{\omega}_D$ are now slowly varying with τ on the basis of the scaling laws illustrated in the previous section, namely, $\bar{k}\sim\rho(\tau)^{-1/2}$, $\gamma_1\sim\rho(\tau)^{-1}$, and $\bar{\omega}_D\sim\rho(\tau)^{-1/2}$. To put it in another way, while for $\gamma=0$ the three-dimensional phase space is trivially reduced to the cylinders $p^2+d^2=\rho^2$, when $\gamma\neq 0$ the cylinders become weakly time dependent and the whole phase space is needed to describe the dynamics. On the other hand, as long as the radial evolution $[\rho(\tau)]$ is slow as compared with the angular one $[\theta(\tau)]$, it is justifiable to examine the latter on short time scales by assuming the former to be fixed.

The bifurcation diagram for Eq. (2.5) in the plane of the control parameters $\bar{\omega}_D$ and γ_1 has been given by various authors, we will refer specifically to the one presented in Ref. 1(c) as their Fig. 3, obtained with $\bar{k}=0.25$. As a matter of fact, inclusion of the dependence on $\bar{k}$ should be needed in order to obtain a better understanding, nonetheless, from the quoted diagram we can extract a qualitative description of the observed transients. Note the following about the diagram: chaos occurs at boundaries between regions of phase locking (of different periodicities); chaos disappears for low driving amplitudes ($\gamma_1 \ll 1$), as well as for high driving frequencies ($\bar{\omega}_D \gg \bar{k}$).

If we then integrate system (2.3) by choosing the parameters such that γ_1 and $\bar{\omega}_D$ lie within the chaotic region in the bifurcation diagram, we expect that for $\tau \ll \gamma^{-1}$ the solution behaves chaotic, then we expect it to sweep different phase-locked states before reaching the steady

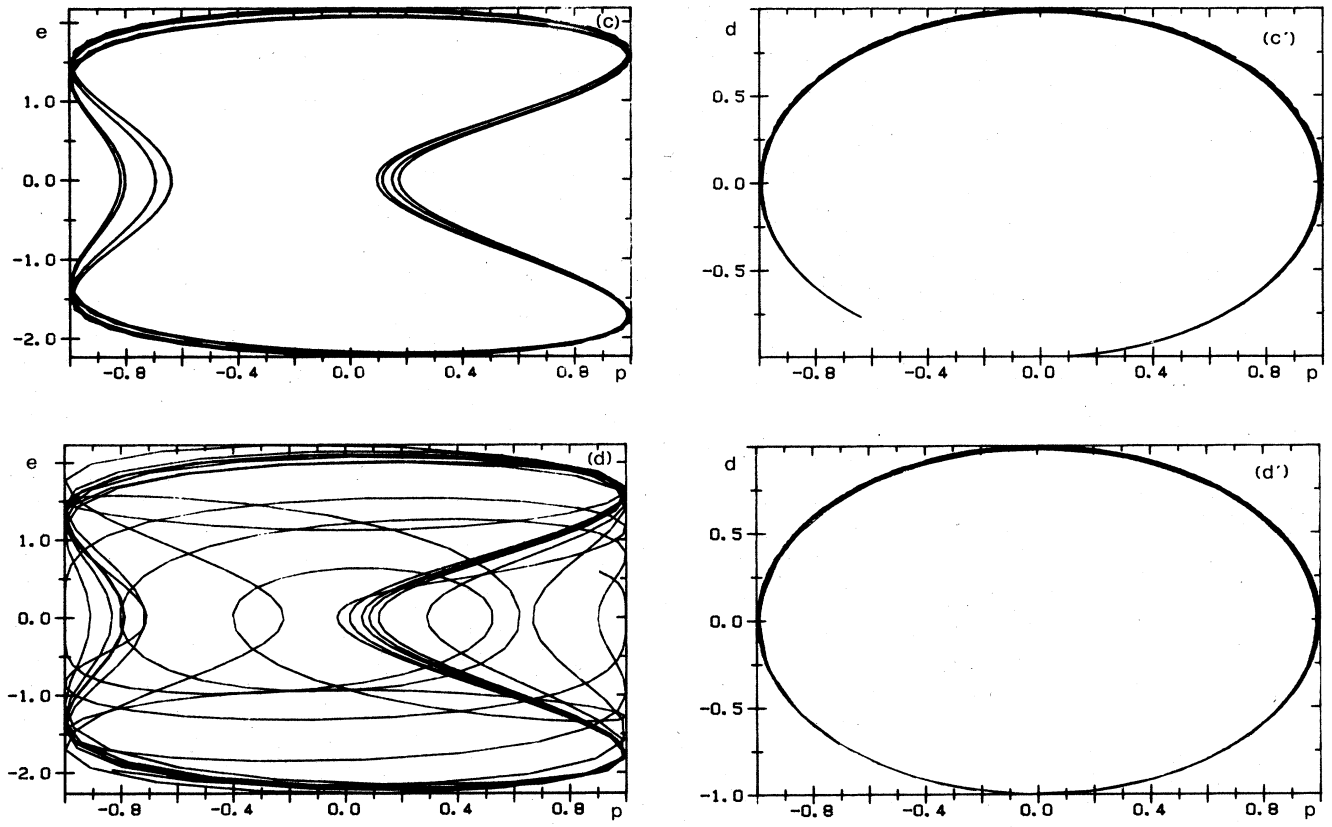

FIG. 1. (*Continued*).

state. Due to the contracting property of (2.3), the overall picture is a cascading through different phase-locked states, starting from a chaotic regime. The steady state is critically dependent, as is clear from the former discussion, on the asymptotic behavior of $\rho(\tau)$. In the numerical results presented in this paper, unless otherwise stated, we always considered $\gamma=10^{-3}$, and $p(0),d(0)$ such that $\rho(0)=1$ [in this case $k'=\bar{k}(0)$, $\omega_D'=\bar{\omega}_D(0)$, and $\gamma_1(0)=2k'a_1$]; we chose the following values for the control parameters: $k'=0.25$, $\omega_D'=0.67$, and $\gamma_1=1.07$, corresponding to a chaotic region for the pendulum. The resulting behavior of $\rho(\tau)$ is displayed in Fig. 2, we can distinguish three regimes: for $\tau\lesssim\gamma^{-1}$, $\rho(\tau)$ decays exponentially, for $\gamma^{-1}\lesssim\tau\lesssim 3\gamma^{-1}$ we have $\rho(\tau)\sim\tau^{\alpha}$ ($\alpha\cong -4.6$), for $3\gamma^{-1}<\tau$ the steady state is reached with $\rho(\tau)\cong\rho_0+\rho_1\cos(\beta\tau)$ ($\rho_0\cong 1.5\times 10^{-3}$, $\rho_1\cong 10^{-4}$).

In the region $\tau\lesssim\gamma^{-1}$, on shorter scales, we observe deviations from a purely exponential decay that can be attributed to phase-locking phenomena on metastable orbits. To get a global picture of the different regimes, we superimposed the phase portraits in the plane (p,e) at various times: in Fig. 3(a) we display the solution from $\tau=900$ to 1000, then from $\tau=1900$ to 2000, and analogously at $\tau=3000$, 4000, and 5000. The solution is initially chaotic then it passes through the expected cascade. The thickness of each orbit is an index of its metastability. To make a direct connection with the pendulum, for the same parameters $\gamma_1=1.07$ and $\omega_D'=0.67$, we integrated system (2.3) with zero atomic damping ($\gamma=0$) by choosing the initial conditions such that ρ was fixed at its previously observed values at $\tau=1000$, 2000, 3000, 4000, and 5000. In Fig. 4(a) we recover a stable chaotic regime, in Fig. 4(b) the period three orbit, in Fig. 4(c) the asymmetric period-one orbit, and in Fig. 4(d) the steady-state limit cycle.

As already pointed out in Sec. II, in this range of pa-

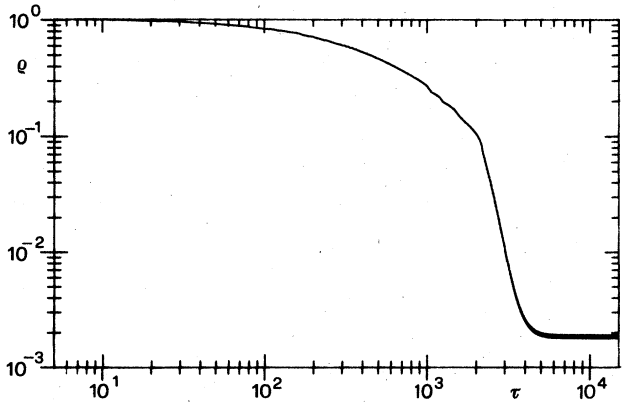

FIG. 2. Log-log plot of $\rho(\tau)$ from integration of Eq. (2.3); $\gamma=10^{-3}$, $k'=0.25$, $\omega_D'=0.67$, $e(0)=p(0)=0$, $d(0)=1$, $a_0=0$, and $\gamma_1(=2k'a_1)=1.07$.

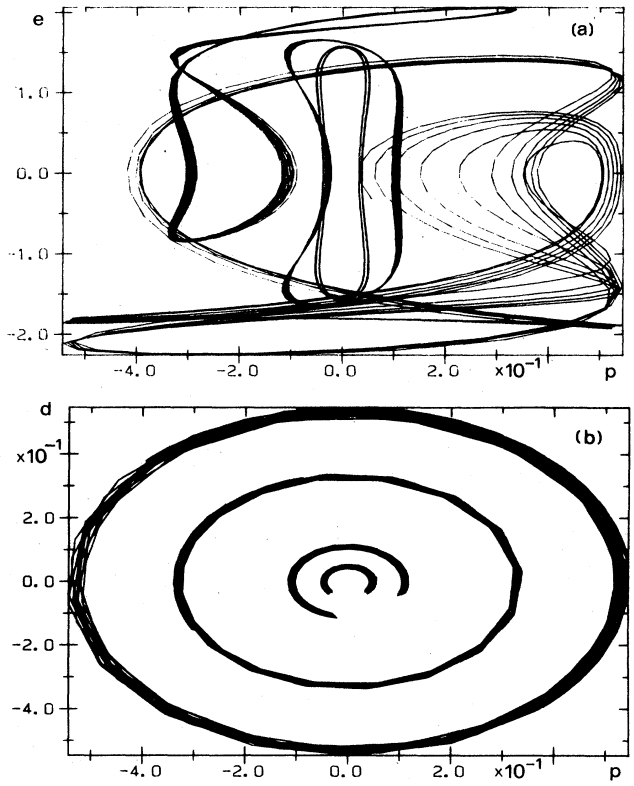

FIG. 3. Same conditions as in Fig. 2. (a) phase portraits in the plane (p,e); (b) phase portraits in the plane (p,d) at times $\tau=1000$, 2000, 3000, 4000, and 5000 (see text).

rameters a degeneracy occurs (with respect to the symmetry $p\rightarrow -p$) in the solutions of (2.3) with $\gamma=0$. In the case $\gamma\neq 0$, when a transition occurs from one metastable attractor to the next one, the "choice" between the two specularly equivalent orbits is critically dependent on the actual phase along the curve $\rho^2=p^2+d^2\cong$const. We observed that this choice is practically unpredictable. By slightly changing the initial conditions along the curve $\rho(0)=1$, we obtained completely different paths in the cascade [compare Fig. 3(a) with 5(a) and 5(b)]; over each phase-locked state the time average $\langle p\rangle$ of the polarization has a well-defined sign, but this sign behaves as a random variable. We can estimate this feature by examining the plot of d versus p in Fig. 3(b), referring to the same initial conditions and time intervals as in Fig. 3(a); clearly, around $\tau=1000$, $\langle p\rangle>0$, while around $\tau=2000$, as well as around $\tau=3000$ and 4000, $\langle p\rangle<0$.

Turning to the pendulum analog, there is a transition from running solutions, in which the pendulum undergoes complete rotations, to the regime of oscillations within a single potential well between $\tau=2000$ and 3000; in this region (see Fig. 2) ρ decays with a power law. Similarly to the cases presented in Figs. 1(b) and 1(c), around $\tau=3000$ the portion of the curve $\rho=$const visited by the orbit is asymmetrical.

IV. ANALYTICAL DESCRIPTION

In making some comments on the structure of the solutions of Eq. (2.3), we start noting that, for a given $e(\tau)$, the first two equations are linear with respect to the atomic variables $p(\tau)$ and $d(\tau)$. For simplicity we consider, as in Sec. III, the case $\gamma'_{\perp}=\gamma'_{\parallel}=\gamma$. As shown in Ref. 8, for the differential operator $\hat{D}$:

$$\hat{D}=\begin{bmatrix} \frac{\partial}{\partial\tau}+\gamma & -\eta(\tau) \\ \eta(\tau) & \frac{\partial}{\partial\tau}+\gamma \end{bmatrix}, \tag{4.1}$$

where $\eta(\tau)$ is a given function, one can construct the Green's function $\mathcal{G}(\tau,\tau')$ in the form:

$$\mathcal{G}(\tau,\tau')=\Theta(\tau-\tau')e^{-\gamma(\tau-\tau')}\begin{bmatrix} \cos(\theta-\theta') & \sin(\theta-\theta') \\ -\sin(\theta-\theta') & \cos(\theta-\theta') \end{bmatrix},$$
$$\theta=\theta(\tau)=\int_0^{\tau}d\tau_1\eta(\tau_1),\quad \theta'=\theta(\tau'),\quad \eta(\tau)=2e(\tau), \tag{4.2}$$

Θ being the step function. The atomic variables $p(\tau)$ and $d(\tau)$ are then given by

$$\begin{aligned} p(\tau)&=\sin\theta(\tau)C(\tau)-\cos\theta(\tau)S(\tau)+\rho(0)e^{-\gamma\tau}\sin\theta(\tau), \\ d(\tau)&=\cos\theta(\tau)C(\tau)+\sin\theta(\tau)S(\tau)+\rho(0)e^{-\gamma\tau}\cos\theta(\tau), \\ S(\tau)&=\gamma\int_0^{\tau}d\tau' e^{-\gamma(\tau-\tau')}\sin\theta(\tau'), \\ C(\tau)&=\gamma\int_0^{\tau}d\tau' e^{-\gamma(\tau-\tau')}\cos\theta(\tau') \end{aligned} \tag{4.3}$$

where $\theta(\tau)$ evolves according to the integro-differential equation

$$\begin{aligned} &\frac{d^2\theta}{d\tau^2}+k'\frac{d\theta}{d\tau}+\rho(\tau)\sin[\theta(\tau)-\alpha(\tau)] \\ &\qquad =2k'[a_0+a_1\cos(\omega'_D\tau)], \\ &\rho(\tau)=\{[\rho(0)e^{-\gamma\tau}+C(\tau)]^2+S^2(\tau)\}^{1/2}, \\ &\alpha(\tau)=\tan^{-1}\left[\frac{S(\tau)}{\rho(0)e^{-\gamma\tau}+C(\tau)}\right]. \end{aligned} \tag{4.4}$$

Equation (4.4) is equivalent to system (2.3); if in general this equivalence is a rather formal one, when $\gamma\ll 1$, it nevertheless allows a quite simple two-time description of the dynamics.

In fact, $\rho(\tau)$ and $\alpha(\tau)$ are actually functions of $\gamma\tau$, so that they vary on the scale γ^{-1}. We then obtain the following picture: superimposed to the pendulum oscillations occurring on time scales $\rho(\tau)^{-1/2}$, on time scales γ^{-1} there is a precession associated with $\alpha(\tau)$, as well as a variation of the pendulum length $\rho(\tau)$. This last effect implies that the degree of cooperativity varies in time; the larger ρ ($\rho\leq 1$), the larger the cooperative behavior of the atoms. In the case considered in Fig. 2, for example, ρ is monotonically decreasing from $\rho(0)=1$ until a limit cycle is reached with $\rho\cong 10^{-3}$: the asymptotic regime is dominated by single-atom scattering. We will see that in the presence of a small bias, $\rho(\tau)$ can exhibit a more exotic behavior. The precession, on the other hand, gives rise, as a memory effect, to a transverse atomic polarization even at $\theta=0$; in fact, assuming oscillations in $\theta(\tau)$ symmetric with respect to $\alpha(\tau)$, we have from (4.3), disregarding the transients, $C(\tau)\sim\cos\alpha(\tau)$ and $S(\tau)\sim\sin\alpha(\tau)$, so that when $\theta(\tau)=0$, $p(\tau)\sim-\sin\alpha(\tau)$.

This phenomenon explains the symmetry breaking dis-

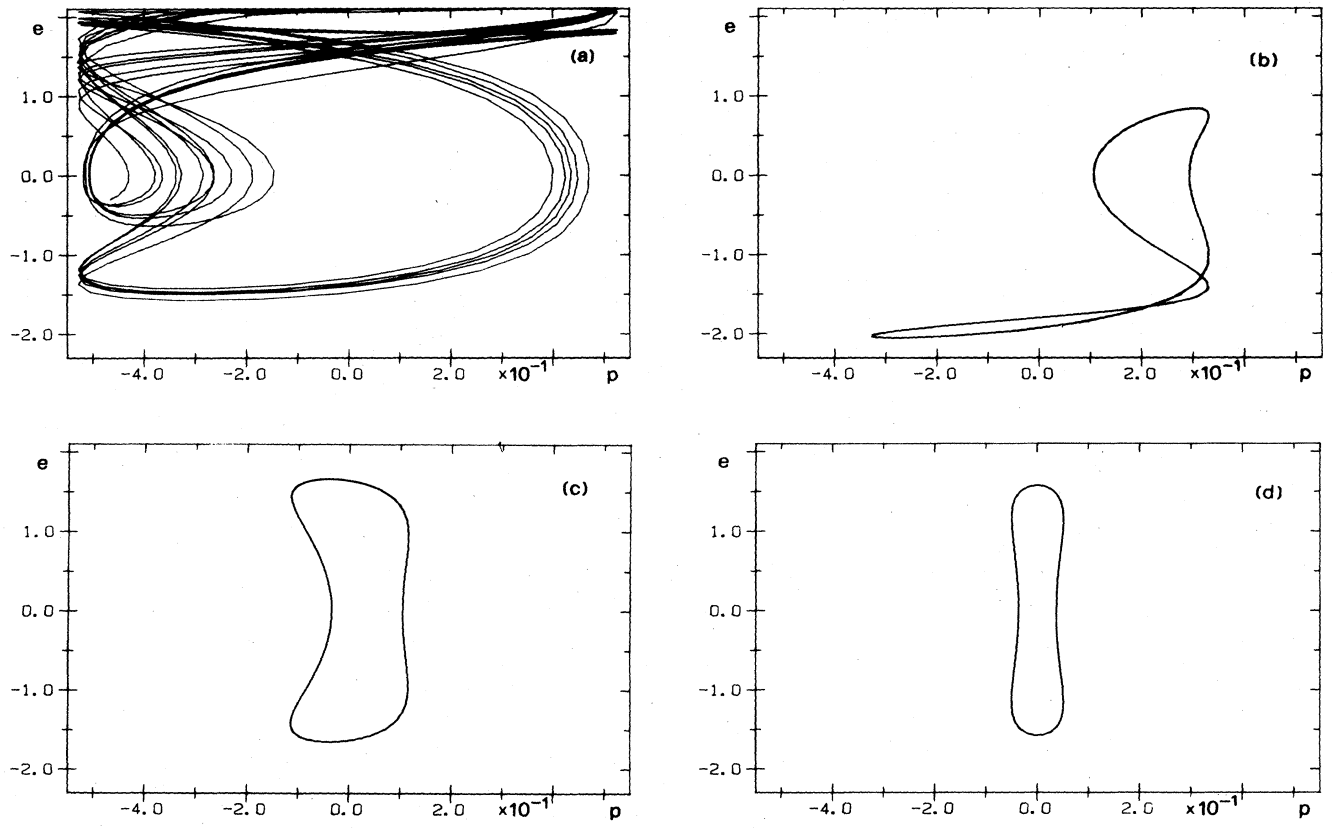

FIG. 4. Phase portraits in the plane (p,e) for $\gamma_{\perp}'=\gamma_{\parallel}'=0$, $k'=0.25$, $\omega_D'=0.67$, and $\gamma_1(=2k'a_1)=1.07$. (a) $e(0)=p(0)=0$, $d(0)=(0.28)^{1/2}$, (b) $e(0)=p(0)=0$ and $d(0)=(0.11)^{1/2}$, (c) $e(0)=p(0)=0$ and $d(0)=(0.0133)^{1/2}$, (d) $e(0)=p(0)=0$ and $d(0)=(0.0026)^{1/2}$.

cussed in the previous section: the pendulum oscillates asymmetrically in the phase plane (p,d). In other terms, the "effective" atomic energy minimum at time τ is $\theta=\alpha(\tau)$ [note that $\alpha(0)=0$]. When, as $\rho(\tau)$ evolves in time, a fixed mode-locked state can no longer be sustained and the system therefore transits to another state, a simple treatment in terms of two time scales is insufficient: we already noted the deviations of $\rho(\tau)$ from a smooth behavior on shorter scales. We expect similar irregularities also for $\alpha(\tau)$. Hence, when degeneracy occurs, as long as the choice between the two equivalent orbits is critically dependent on $\alpha(\tau)$, such a choice appears to be a random one, as shown in Figs. 3(a), 5(a), and 5(b). Of course, a better understanding of this phenomenon can only be obtained with a complete statistical analysis of the initial data along the curve $\rho(0)=1$.

We will now show how one can obtain an approximate description of the dynamics over the time scales γ^{-1} through a sequence of pendulum equations. First note that, due to the exponential factors in the integrals (4.3), the functions $\rho(\tau)$ and $\alpha(\tau)$ depend uniquely on the earlier evolution up to $\tau-\gamma^{-1}$; we have approximately

$$S(\tau)\simeq\bar{S}(\tau)=\gamma\int_{\tau-\gamma^{-1}}^{\tau}d\tau'\sin\theta(\tau')\ ,$$
$$C(\tau)\simeq\bar{C}(\tau)=\gamma\int_{\tau-\gamma^{-1}}^{\tau}d\tau'\cos\theta(\tau')\ . \tag{4.5}$$

Over the interval $0<\tau<\gamma^{-1}$, we approximate (4.4) with

$$\frac{d^2\theta_0}{d\tau^2}+k'\frac{d\theta_0}{d\tau}+\rho(0)\sin\theta_0=2k'[a_0+a_1\cos(\omega_D'\tau)] \tag{4.6}$$

Over the next interval $\gamma^{-1}<\tau<2\gamma^{-1}$ we will have

$$\rho_1=[\bar{C}^2(\gamma^{-1})+\bar{S}^2(\gamma^{-1})]^{1/2}\ ,$$
$$\alpha_1=\tan^{-1}\left[\frac{\bar{S}(\gamma^{-1})}{\bar{C}(\gamma^{-1})}\right]\ ,$$
$$\frac{d^2\theta_1}{d\tau^2}+k'\frac{d\theta_1}{d\tau}+\rho_1\sin(\theta_1-\alpha_1)=2k'[a_0+a_1\cos(\omega_D'\tau)]\ , \tag{4.7}$$

the time averages $\bar{S}(\gamma^{-1})$ and $\bar{C}(\gamma^{-1})$ referring to the solution $\theta_0(\tau)$ of Eq. (4.6). Upon iterating this procedure we obtain a sequence ρ_n,α_n giving the coarse-grained evolution of the functions $\rho(\tau)$ and $\alpha(\tau)$. We stress that the more the time law $\theta_{n-1}(\tau)$ is asymmetrical with respect to the reflection $\theta\rightarrow-\theta$, the more ρ_n and α_n differ from zero [see Eq. (4.5)].

We conclude this section with two remarks. First we note that, as shown in Ref. 8, one can reduce system (2.3) to a single integro-differential equation, also in the case $\gamma_{\parallel}'\neq\gamma_{\perp}'$; the treatment becomes technically more compli-

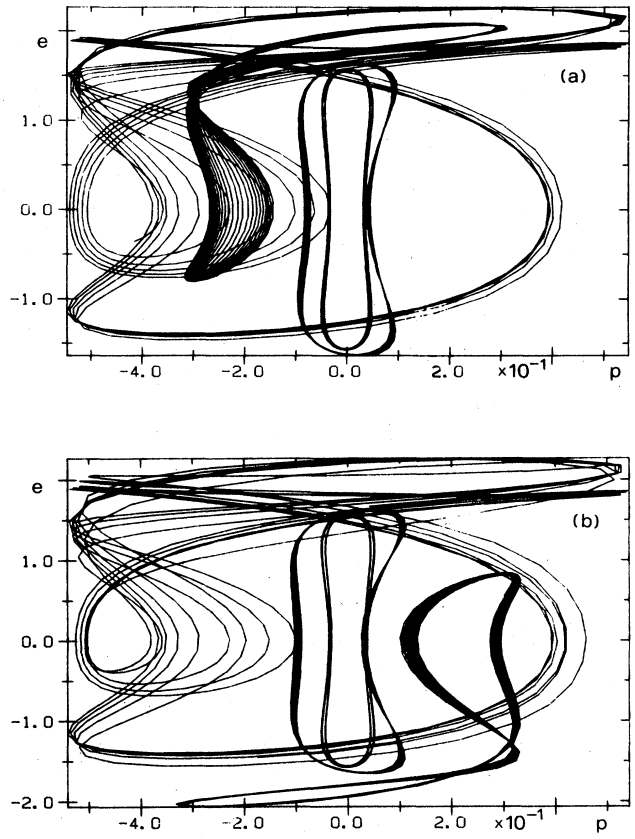

FIG. 5. Phase portraits in the plane (p,e) with $\gamma=10^{-3}$, $k'=0.25$, and $\omega'_D=0.67$, (a) $e(0)=0$ and $d(0)=p(0)=(0.5)^{1/2}$, (b) $e(0)=0$, $d(0)=0.95$, and $p(0)=[1-d^2(0)]^{1/2}$.

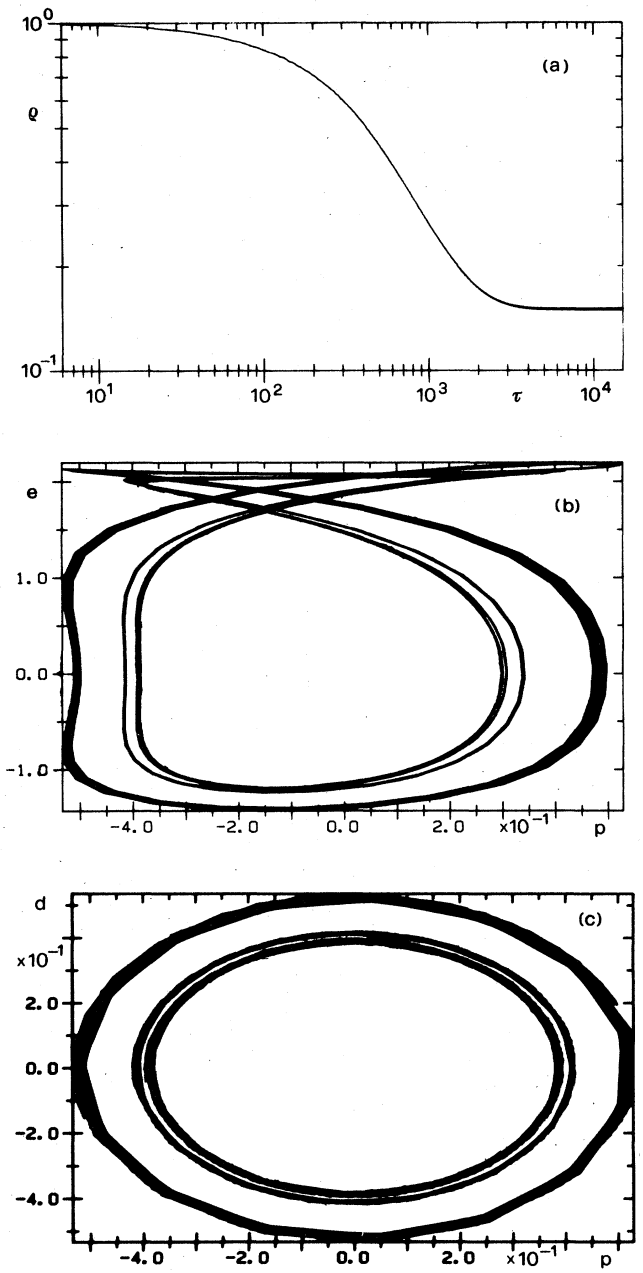

FIG. 6. $\gamma=10^{-3}$, $k'=0.25$, $\omega'_D=0.67$, $\gamma_0(=2k'a_0)=0.1$, $\gamma_1(=2k'a_1)=1.07$, $e(0)=p(0)=0$, and $d(0)=1$. (a) log-log plot of $\rho(\tau)$, (b) phase portraits in the plane (p,e) at times $\tau=1000$, 2000, 3000, 4000, and 5000, (c) same as in (b) but in the plane (p,d).

cated but we do not expect particularly different features, at least when $\gamma'_{||}$ and $\gamma'_{\perp}$ are of the same order.

The second remark refers to the asymptotic regime when $\rho \ll 2k'a_0, 2k'a_1$. The third equation in (2.3) becomes in this case linear, and for $\theta(\tau)$ we have

$$\theta(\tau) \sim (2k'a_1/\omega'_D)\cos(\omega'_D\tau)+2a_0\tau \quad (\tau \gg 1) .$$

The atomic variables $p(\tau)$ and $d(\tau)$, as one sees from (4.3), being periodic functions of $\theta(\tau)$, *a priori* involve infinitely many frequencies; in the limit case $2k'a_1/\omega'_D \ll 1$, $a_0 \neq 0$ one recovers the resonance fluorescence behavior.

V. NUMERICAL RESULTS IN THE CASE WITH BIAS

With a purely oscillatory driving force, as previously noted, there is degeneracy with respect to the symmetry $p \rightarrow -p$ in the solutions of (2.3): in the cascading process stochasticity tends to restore the symmetry. As a consequence, atomic cooperativity decreases with time and, according to the discussion of Sec. III, a region of high effective driving frequency is reached where chaos disappears. In order to remove the degeneracy, we now add a bias to the driving force: we expect an enhancement of cooperativity at steady state.

As always, we choose initial values of p and d on the curve $\rho=1$ and keep for the control parameters the same values as in Sec. III; we examine the behavior of the system for values of the bias $\gamma_0=2k'a_0$ smaller than the fixed driving amplitude. In Fig. 6(a) we exhibit the function $\rho(\tau)$ in the case $\gamma_0=0.1$. Apart from some irregularities related to phase-locking phenomena, $\rho(\tau)$ decays

smoothly to a steady state with a constant amplitude $\rho_0 \cong 1.6\times10^{-1}$ and an oscillating amplitude $\rho_1 \ll \rho_0$; note that in the corresponding case with $\gamma_0=0$ (Fig. 2), a power-law behavior was clearly appearing before reaching the asymptotic regime, and that we had then $\rho_0 \cong 1.5\times10^{-3}$. Thus, the presence of a bias actually favors the survival of cooperativity (in our case the bias is of the order 10% of the driving amplitude). Figure 6(b) refers to (p,e) phase portraits taken, as in Fig. 3(a), every 1000 units of time. Apart from a small contraction, we always observe the same structure (the orbit at $\tau=5000$ is superimposed to the one at 4000 because then the steady state is already reached).

The asymmetry of the orbit is also maintained asymptotically in this case, while for $\gamma_0=0$ symmetry was restored [see Fig. 3(a)]. In Fig. 6(c), for the same time intervals considered in Fig. 6(b), we display d versus p. Note that contrary to the case $\gamma_0=0$, we always deal with solutions lying outside the first potential well of the pendulum. In other words, the constant-amplitude part of the incident field is large enough to sustain the emission also when the system is totally inverted. We can infer that the power-law behavior observed for $\rho(\tau)$, when $\gamma_0=0$, was associated to the decay through the separatrix orbit. In the plane (p,d) the orbit is a symmetric one, but it is passed through with a quite complicated time law; we notice that the time average of p is clearly different from zero (in the present case $\langle p \rangle < 0$). Another effect of the bias is a stronger dependence on the initial phase of the Bloch vector. In fact, the deformation introduced in the potential of the pendulum [$V(\theta)=-\cos\theta-\gamma_0\theta$] is such that a variation of the initial conditions along the curve $\rho=1$ actually corresponds to a large variation of the pendulum energy; this is confirmed by the numerical results. Figure 6 refers to $p(0)=e(0)=0$, $d(0)=1$; if one chooses instead $p(0)=d(0)=(0.5)^{1/2}$, $e(0)=0$, one obtains quite a different behavior (see Fig. 7). The plot of $\rho(\tau)$, shown in Fig. 7(a), exhibits a discontinuity in the first derivative at approximately $\tau=10$.[3] The origin of this singularity is understood from Fig. 7(b), in which we superimposed the phase portraits related to the following time intervals: $400 \le \tau \le 500$, $900 \le \tau \le 1000$, and analogously at $\tau=1500$, 2000, and 2500. The three smallest orbits refer to the last three intervals: we are approaching the same steady state exhibited in Fig. 6(b). The two largest orbits refer to the first two time intervals, apart from a stronger contraction they have the same structure as the orbits of Fig. 6(b) but they are specularly inverted.

The initial phase mismatch with the steady-state behavior, mode locked with the driving term, is overcome with an abrupt transition around $\tau=1000$. Other attempts made by varying the initial data along the curve

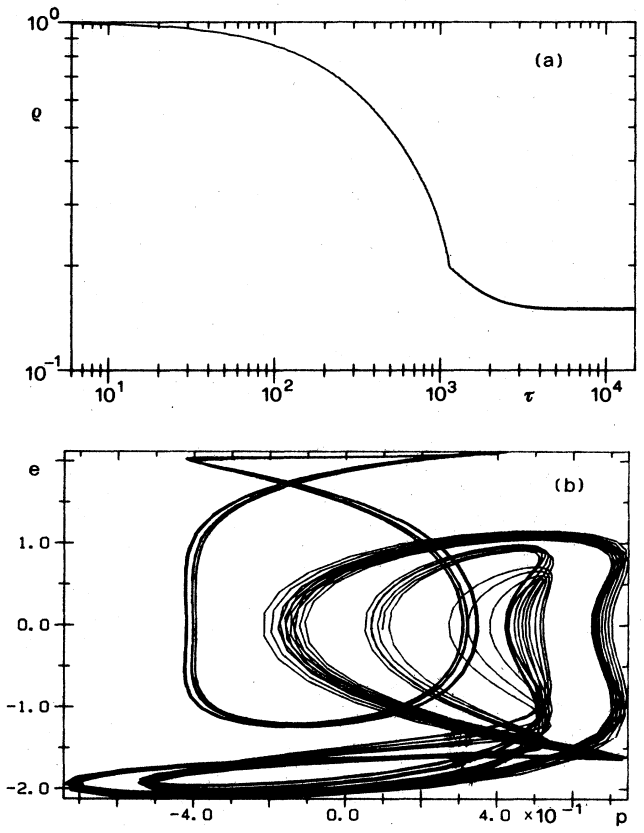

FIG. 7. Same parameters as in Fig. 6 but with different initial conditions; $e(0)=0$ and $p(0)=d(0)=(0.5)^{1/2}$. (a) log-log plot of $\rho(\tau)$; (b) phase portraits in the plane (p,e) at times $\tau=500$, 1000, 1500, 2000, and 2500.

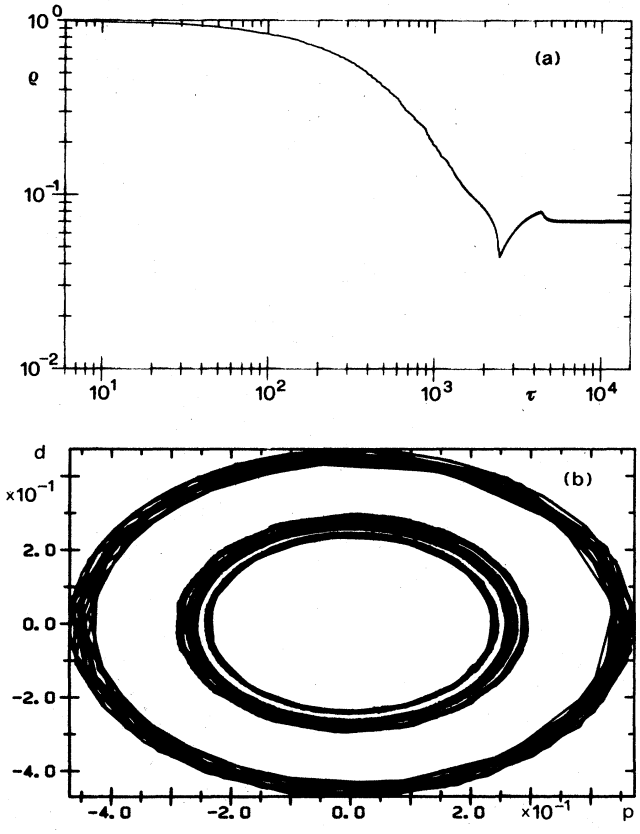

FIG. 8. $\gamma=10^{-3}$, $k'=0.25$, $\omega_D'=0.67$, $\gamma_0(=2k'a_0)=0.3$, $\gamma_1(=2k'a_1)=1.07$, $e(0)=p(0)=0$, and $d(0)=1$. (a) log-log plot of $\rho(\tau)$, (b) phase portraits in the plane (p,d) at times $\tau=1000$, 2000, 3000, 4000, and 5000.

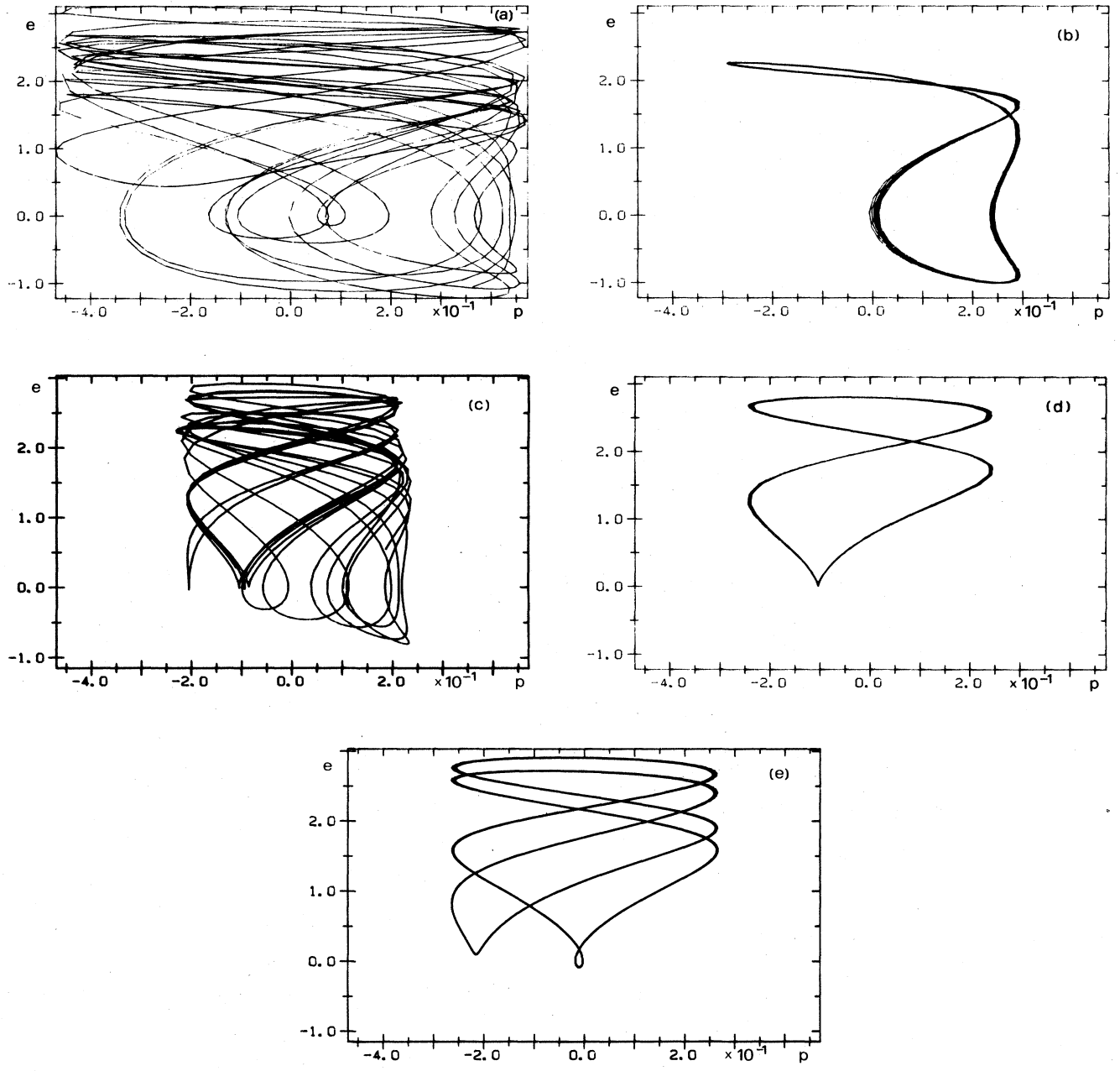

FIG. 9. Same parameters as in Fig. 8, (p,e) portraits, (a) $\tau=1000$, (b) $\tau=2000$, (c) $\tau=2500$, (d) $\tau=3000$, (e) $\tau=12\,500$.

$\rho=1$ resulted in slight variations of the two main scenarios presented above.

So far we reported on cases in which $\rho(\tau)$ monotonically decreases. The long time-scale behavior of $\rho(\tau)$ is regulated by atomic dephasings, and a decay on times of the order γ^{-1} is expected; on the other hand, the evolution of $\rho(\tau)$ is influenced, through memory effects, by the amount of $\rho(\tau)$ is asymmetry of the solution. The stronger the asymmetry, the stronger the survival of cooperativity; we actually observed, for a larger value of γ_0 ($\gamma_0=0.3$), a transient in which asymmetry overcomes the incoherent processes. In this case $\rho(\tau)$ decreases up to $\tau\cong2500$, then, after a cusp, it increases up to $\tau\cong4000$ where again its derivative is discontinuous, then eventually stabilizes to a mode-locked orbit with constant amplitude $\rho_0\cong7\times10^{-2}$ [see Fig. 8(a)]. Figure 8(b) is the analog of Fig. 6(c) (plot of d versus p every 1000 units of time). The largest orbit is at $\tau=1000$, the second largest is at $\tau=2000$, the smallest is at $\tau=3000$, and in between these two lie, almost coincident, the orbits at $\tau=4000$ and 5000. We note furthermore that the larger bias enhances the irregular behavior of $\rho(\tau)$ on short time scales; this is particularly

clear in the range $10^2 \leq \tau \leq 10^3$. If we relate this staircase behavior to high periodicity phase lockings, we can infer that the bias has the effect of stabilizing the phase-locked states, a feature already noted[1(c)] for the pendulum case.

The two discontinuities in the derivative of $\rho(\tau)$ can be associated to abrupt structural changes in the form of the orbit. In Fig. 9 we display phase portraits in the plane (p,e) at different times, in each case the evolution being followed for 100 units of time. Figure 9(a) is taken at $\tau=1000$, and we are still in a chaotic regime. At $\tau=2000$ [Fig. 9(b)] we have a period three orbit, strongly asymmetrical; at $\tau=3000$ [Fig. 9(d)] the cusp of $\rho(\tau)$ has been passed through and a new orbit has appeared, structurally distinct from the previous one. At $\tau \cong 2500$ [Fig. 9(c)] close to the cusp, when $\rho(\tau)$ rapidly sweeps different phase-locked orbits, we can characterize the behavior as chaotic transient. Up to $\tau \cong 4000$ we observed essentially the same orbits as in Fig. 9(d); the second discontinuity in the derivative of $\rho(\tau)$, at $\tau=4000$, corresponds to a period doubling, to an orbit to become the steady state. Figure 9(e) refers to $\tau=12\,500$ at steady state, but at $\tau=5000$ we already observed essentially the same shape.

We considered larger values of γ_0 ($\gamma_0=0.4,0.5,1$), and $\rho(\tau)$ reproduced the behavior described for $\gamma_0=0.1$ in Fig. 6; higher values of γ_0 resulted in orbits of higher periodicity; in all cases strong asymmetry was observed. Hence, in general, the bias sustains the cooperativity resulting in a steady state with a relatively high ρ_0 and a superimposed oscillation of amplitude $\rho_1 \ll \rho_0$; so far we have not been able to fully understand the physical mechanism responsible for the restoration of atomic coherence observed in the case $\gamma_0=0.3$.

VI. CONCLUDING REMARKS

We presented an analysis of the behavior of a high-density gas of two-level atoms in a cavity, driven by a coherent amplitude-modulated field, looking for the feasibility of an experiment on the quasiperiodicity route to chaos. We obtained that, provided the cooperation time τ_c is much smaller than the atomic decay times, chaos can be observed as a transient; we have not been able to find chaos at steady state, but we have no *a priori* reason to exclude this possibility. A more complete numerical analysis or a treatment along the lines of Melnikov's method[9] will be needed to have a conclusive answer on this point. Nonetheless, if the system is prepared in such a way as to obtain a cooperation time τ_c of, say, the order of nanoseconds, while keeping the decay times in the order of hundreds of nanoseconds, the time-dependent spectrum[10] of the output signal is expected to exhibit chaotic character in the region of frequencies centered around τ_c^{-1}. The amplitude-modulated signal in such a case can be realized by a mode-locked, synchronously pumped cw dye laser.

When the chaotic transient is over, a cascading process occurs through different phase-locked states. While, in the absence of bias, stochasticity adds to incoherent processes that tend to destroy atomic cooperativity, with bias the survival of cooperativity is favored even at steady state, up to 10% of the initial value. This effect is a direct consequence of removal of degeneracy of the orbits, leading to stronger asymmetry, as explained in the previous sections. The asymmetry has its counterpart in a transmitted field $e(t)$ oscillating around a constant value $\langle e \rangle$, different from zero also without a bias.

In the absence of an injected signal, it is known[3(a)] that the system can produce squeezed states, if prepared in such a way as to oscillate along orbits close to the separatrix of the pendulum. It is reasonable to infer that such orbits can in fact be stabilized by a small oscillating driving field. A complete characterization of the observed transient chaos as well as an analysis of quantum effects are left for future work.

ACKNOWLEDGMENTS

We thank Hyatt Gibbs for his support and hospitality at the Optical Sciences Center of the University of Arizona. One of us, V.G.B., also acknowledges useful discussions with David McLaughlin, Thomas Bohr, and David Rand, and S.W.K. thanks the Deutsche Forschungsgemeinschaft (DFG) for financial support.

[1](a) B. A. Huberman, J. P. Crutchfield, and N. H. Packard, Appl. Phys. Lett. **3**, 750 (1980); (b) N. F. Pedersen, and A. Davidson, *ibid.* **39**, 830 (1981); (c) D. D'Humières, M. R. Beasley, B. A. Huberman, and A. Libchaber, Phys. Rev. A **26**, 3483 (1982).

[2]S. Haroche, in *New Trends in Atomic Physics,* edited by G. Grynberg and R. Stora (North-Holland, Amsterdam, 1984), and references therein.

[3](a) A. Heidmann, J. M. Raimond, and S. Reynaud, Phys. Rev. Lett. **54**, 326 (1985); (b) D. F. Walls, Nature **306**, 141 (1983).

[4](a) T. Yamada and R. Graham, Phys. Rev. Lett. **45**, 1322 (1980); (b) F. T. Arecchi, G. L. Lippi, G. P. Puccioni, and J. R. Tredicce, Opt. Commun. **51**, 308 (1984).

[5]F. T. Arecchi and E. Courtens, Phys. Rev. A **2**, 1730 (1970).

[6]R. Bonifacio and L. A. Lugiato, Opt. Commun. **19**, 172 (1976).

[7]A. Nordsieck, Math. Comput. **16**, 22 (1962).

[8]V. G. Benza and E. Montaldi, Phys. B **45**, 259 (1982).

[9]V. K. Melnikov, Trans. Moscow Math. Soc. **18**, 1 (1963).

[10]J. H. Eberly and K. Wodkiewicz, J. Opt. Soc. Am. **67**, 1252 (1977).